EPSC Abstracts
Vol. 13, EPSC-DPS2019-1852-1, 2019
EPSC-DPS Joint Meeting 2019

EPSC
EPSC-DPS Joint Meeting 2019
15–20 September 2019 | Geneva, Switzerland

Cumberland and Rocknest analogues near-infrared and LIBS measurements compared to MSL

Jérémie Lasue (1), Erwin Dehouck (2), Jeffrey R. Johnson (3), Pierre Beck (4), Gaël David (1), Caroline Freissinet (5), Heather V. Graham (6), Christine A. Knudson (6), Lisa Krämer Ruggiu (7), Danika F. Wellington (8), Jim F. Bell (8), Kevin M. Cannon (9), Olivier Forni (1), Olivier Gasnault (1), Stéphane Le Mouélic (10), Nicolas Mangold (10), Pierre-Yves Meslin (1), Sylvestre Maurice (1), Roger C. Wiens (11)
(1) IRAP-OMP, CNRS-UPS, Toulouse, France (jlasue@irap.omp.eu), (2) LGL-TPE, Université de Lyon, France, (3) Johns Hopkins University APL, Laurel, MD, USA, (4) IPAG, Grenoble, France, (5) LATMOS-IPSL, Guyancourt, France, (6) NASA Goddard, Greenbelt, MD, USA, (7) CEREGE, Aix-en-Provence, France, (8) SESE, ASU, Tempe, AZ, USA, (9) University of Central Florida, Orlando, USA, (10) LPG, CNRS, Nantes, France, (11)LANL, NM, USA,

Abstract

Analogues of the Rocknest (RN) windblown deposit (sol 84) and Cumberland (CB) mudstone drill fines (sol 281) have been generated in the laboratory based on the mineralogical information retrieved by MSL. Here, we report initial results of the near-infrared analysis of these analogues compared to the MSL measurements made of the targets on Mars.

1. Introduction

ChemCam is a Laser-Induced Breakdown Spectroscopy (LIBS) instrument on-board the NASA Mars Science Laboratory (MSL) rover that has been exploring Gale Crater, Mars for the past six years [1, 2]. Its spectrometric capability can be used to retrieve reflectance signals from martian surfaces of interest in the 400-840nm region which can show spectral features of iron-bearing oxides, pyroxenes, and calcium sulphates [3, 4]. Similarly, the rover's Mastcam CCD cameras (1600×1200 pixel) use an 8-position filter wheel of broadband near-infrared cut-off filter for RGB Bayer imaging and twelve narrow band geology filters distributed between the two cameras, spanning the 445-1013 nm wavelength range [5, 6].

2. Analogue samples

The mineralogical understanding of martian rocks and regolith have dramatically improved thanks to the use of X-Ray Diffraction by the CheMin instrument on the Curiosity rover [7]. A new generation of Mars simulants is being generated based on MSL's mineralogical analyses to provide further understanding of these materials in the laboratory.

The mineralogy of RN (26 wt.% plagioclase, 20 wt.% pyroxene, 13 wt.% olivine, 2 wt.% magnetite, 1 wt.% hematite [8, 9]) was used to generate the Mars Global Simulant-1 (MGS-1) analogue [10]. The simulant grain size is < 1 mm and its spectral properties have been favourably compared to both rover and orbiter observations of Mars soils [10].

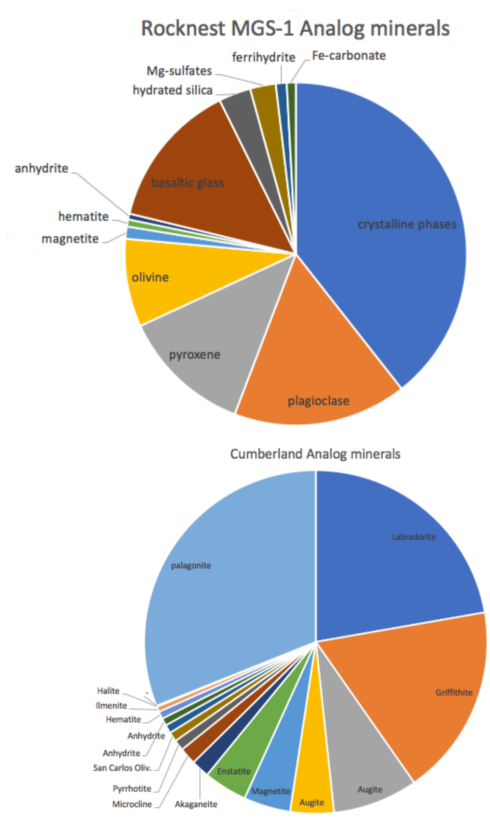

Figure 1: *Mineralogy of the CB and Rocknest analogues [10, 11, 12].*

Similarly, the mineralogy CB [11] (which is broadly similar to Rocknest, but contains less abundant olivine and ~20 wt.% smectite clays) was used to generate a simulant of this mudstone composition by the SAM team, which is described in Fig. 1 to compare with the SAM instrument measurements [12, 13]. Since the CB analogue sample is a powder (grain size < 150 µm), we chose to compare its spectral properties with those of the tailings produced by the MSL drill when it acquired the sample.

3. Results for the infrared

Infrared reflectance spectra were measured using the spectro-gonio-radiometer available at the IPAG in Grenoble [14]. Bidirectional reflectance spectra were measured with a photometric accuracy below 1% in the 0.5–3.0 µm range with a sampling interval of 10 nm. Fig. 2 presents the infrared spectra obtained for the two samples compared to Mastcam's observations of Rocknest scoop 4 and ChemCam's observations of Rocknest scoop 2 Kenyon soils (sol 97) and the observations of the Cumberland drill hole tailings [3, 6]. The three types of measurements follow the same trends.

The CB analogue exhibits greater reflectance > 600 nm than the RN analogue, which agrees with the Mastcam spectra. The CB analogue also displays a less prominent ferric absorption near 535 nm than the RN analogue, likely resulting from the use of palagonite to represent its amorphous component. The ChemCam passive spectra of the martian targets also show that CB has a weaker ferric absorption and a higher relative reflectance than RN. The variations in overall albedo for this target likely result from a combination of dust cover, surface texture, and photometric effects.

The greater band depth at 1.9 µm in the CB analogue is peculiar, since RN and CB are supposed to have similar amounts of H_2O based on SAM measurements (~2 wt.% [15]). Note that the water content of the CB analogue was not monitored for practical reasons. While we took care to keep the samples under dehydrated conditions, this may indicate that some mineral phases present in the CB analogue sample (e.g., smectite, palagonite) are more hydrated than their martian counterparts. This could also be related to variations in grain size of the hydrated phases in the mixtures.

The bands around 1.4 and 1.9 microns in the CB spectrum are mainly due to the presence of the ferroan saponite griffithite used in the mixture (Fig. 2). Also, the metal-OH bands associated with smectites around 2.3 µm are not obvious. This is a reminder that clay minerals within complex mixtures may not be easy to detect from orbit, even at the ~20 wt.% level and without dust cover.

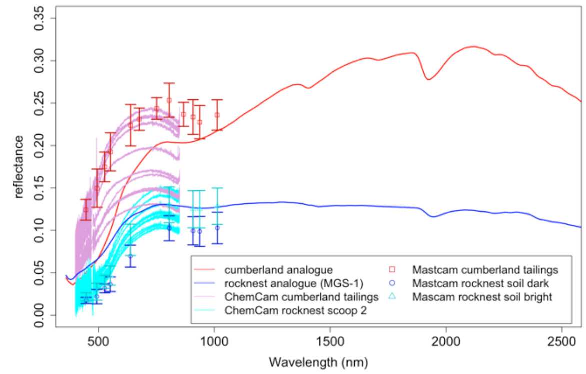

Figure 2: *Comparison of the reflectance spectra for CB and RN analogues with the ones measured by CCAM and Mastcam.*

4. Conclusions

The Cumberland and Rocknest analogues are spectrally distinct, with the CB analogue being brighter and showing stronger OH/H_2O absorption signatures. Still, these two analogues do not appear to reproduce entirely the differences observed in passive observations of the actual (martian) RN and CB samples. The analogues will be analyzed with active LIBS before the summer and the results will be presented at the conference.

Acknowledgements

Support from CNES and NASA's Mars Program Office are acknowledged.

References

[1] Maurice *et al.* (2012) SSR, DOI 10.1007/ s11214-012-9902-4 [2] Wiens *et al.* (2012) SSR, DOI 10.1007/s11214-012-9912-2 [3] Johnson *et al.* (2015) Icarus, DOI j.icarus.2014.02.028 [4] Johnson *et al.* (2019) LPSC #2132 [5] Bell *et al.* (2012) *LPSC* #1659. [6] Wellington *et al.* (2017). *American Mineralogist*, *102*(6), 1202-1217. [7] Blake et al. (2012) *Space, Sci., Rev.*, *170*(1-4), 341-399 [8] Bish *et al.* (2013) Science, DOI 10.1126/science.1238932 [9] Achilles *et al.* (2017) Icarus, DOI 10.1002/2017JE005262 [10] Cannon *et al.* (2019) Icarus, DOI j.icarus.2018.08.019 [11] Vaniman D. T. et al. (2014) *Science, 343*. [12] Stern *et al.* (2018) AGU P51C-15B [13] Knudson *et al.* (2019), LPSC # 2489 [14] Potin *et al.* (2018) Applied Optics, DOI 10.1364/AO.57.008279 [15] Sutter *et al.* (2017) *JGR, DOI: 10.1002/2016JE005225*.